Aging and memory effects in superparamagnets and superspin glasses

M. Sasaki, P. E. Jönsson, and H. Takayama
Institute for Solid State Physics, University of Tokyo, 5-1-5 Kashiwa-no-ha, Kashiwa, Chiba 277-8581, Japan

H. Mamiya
National Institute for Materials Science, Sengen 1-2-1, Tsukuba, Ibaraki 305-0047, Japan
(Received 24 June 2004; published 7 March 2005)

Many dense magnetic nanoparticle systems exhibit slow dynamics which is qualitatively indistinguishable from that observed in atomic spin glasses and its origin is attributed to dipole interactions among particle moments (or superspins). However, even in dilute nanoparticle systems where the dipole interactions are vanishingly small, slow dynamics is observed and is attributed solely to a broad distribution of relaxation times which in turn comes from that of the anisotropy energy barriers. To clarify characteristic differences between the two types of slow dynamics, we study a simple model of a noninteracting nanoparticle system (a superparamagnet) analytically as well as ferritin (a superparamagnet) and a dense Fe_3N nanoparticle system (a superspin glass) experimentally. It is found that superparamagnets in fact show aging (a waiting time dependence) of the thermoremanent magnetization as well as various memory effects. We also find some dynamical phenomena peculiar only to superspin glasses such as the flatness of the field-cooled magnetization below the critical temperature and memory effects in the zero-field-cooled magnetization. These dynamical phenomena are qualitatively reproduced by the random energy model, and are well interpreted by the so-called droplet theory in the field of spin-glass study.

DOI: 10.1103/PhysRevB.71.104405 PACS number(s): 75.10.Nr, 75.40.Gb, 75.50.Tt, 75.50.Lk

I. INTRODUCTION

One of the most attractive topics in the field of condensed matter physics is slow dynamics such as nonexponential relaxation, aging (a waiting time dependence of observables),[1,2] and memory effects. These phenomena are observed in various systems like polymers,[1,3,4] high-T_c superconductors,[5] granular materials,[6] and spin glasses. Especially in the field of spin glasses, slow dynamics has been studied widely both experimentally[2,7–9] and theoretically[10–15] to examine the validity of novel concepts of spin glasses such as a hierarchical organization of states[16,17] and temperature chaos.[18–21] These extensive studies have revealed various interesting behaviors in dynamics like the coexistence of memory and rejuvenation.[7–9] Such findings have stimulated many researchers to study slow dynamics in various systems like geometrically frustrated magnets,[22,23] transition-metal oxides,[24] orientational glasses,[25,26] supercooled liquids,[27] and dense magnetic nanoparticle systems[28–33] by using experimental protocols developed in the study of spin glasses. Magnetic nanoparticle systems, which we study in this paper, are of current interest because of their significance for technological applications as well as for their fundamental magnetic properties.[34]

In magnetic nanoparticle systems, there are two possible origins of slow dynamics. The first one is a broad distribution of relaxation times originating solely from that of the anisotropy energy barriers of each nanoparticle moment. This is the only source of slow dynamics for sparse (weakly interacting) magnetic nanoparticle systems, in which the nanoparticles are fixed in space. We hereafter call the magnetic moments of each nanoparticle *superspins*, and such weakly interacting magnetic nanoparticle systems *superparamagnets*. However, for dense magnetic nanoparticle systems, there is a second possible origin of slow dynamics, namely, cooperative spin-glass dynamics due to frustration caused by strong dipolar interactions among the particles and randomness in the particle positions and anisotropy axis orientations.[35] In fact, evidence for a spin-glass transition such as the critical divergence of the nonlinear susceptibility has been found in dense magnetic nanoparticle systems.[36–38] We hereafter call such dense magnetic nanoparticle systems, which exhibit spin-glass behavior, *superspin glasses*.

Now the point is that magnetic nanoparticle systems involve two possible mechanisms for slow dynamics, and which of the two is relevant depends essentially on the concentration of nanoparticles. Then, in order to understand appropriately slow dynamics in magnetic nanoparticle systems, it is desirable to clarify which observed phenomena are simply due to slow dynamics caused by a broad distribution of relaxation times, and which ones are brought by cooperative dynamics peculiar to superspin glasses. For this purpose, we first study a simple model of noninteracting magnetic nanoparticle systems (superparamagnets) analytically. As a consequence, we find that even superparamagnets exhibit aging of the thermoremanent magnetization and various memory effects. In particular, we show that the curious memory effects recently reported by Sun *et al.*,[39] which were claimed to give evidence of the existence of a superspin glass phase, can be understood simply as superparamagnetic relaxation (see also Refs. 40–42).

We also perform experiments on ferritin (a superparamagnet[43,44]) and a dense Fe_3N nanoparticle systems (a superspin glass[29,37,45,46]). The results for ferritin are qualitatively similar to those of our simple model of superparamagnets. The comparison of the phenomena observed in the superparamagnet and the superspin glass reveals some properties peculiar only to superspin glasses, e.g., the flat-

ness of the field-cooled magnetization below the critical temperature and memory effects in the zero-field-cooled magnetization. Particularly, the former phenomenon reminds us of Parisi's equilibrium susceptibility in the spin-glass mean-field theory.[47] However, we propose an interpretation based on the spin-glass droplet theory[20,48] which predicts the instability of the spin-glass phase under a static magnetic field of any strength and so claims the observed field-cooled magnetization to be a property far from equilibrium.[49] We also show that these experimental results peculiar to superspin glasses are qualitatively reproduced by the random energy model.[50–52]

The outline of the present manuscript is as follows. In Sec. II we introduce a model of superparamagnets and report aging and memory effects observed in this model. The results of experiments on ferritin are also shown in this section. In Sec. III we show experimental results on a dense Fe_3N nanoparticle system. Some properties found only in the superspin glass are interpreted by the random energy model and the droplet theory. Section IV is devoted to a summary.

II. SLOW DYNAMICS IN SUPERPARAMAGNETS

A. Model and master equation approach

Here we adopt a simple model which is considered to describe the essential slow dynamics in noninteracting magnetic nanoparticle systems (superparamagnets). The magnetic moment (superspin) of one nanoparticle, which does not interact with any other superspins, is supposed to occupy one of two states with energies $-KV \pm hM_sV$, where K is the bulk anisotropy constant, V the volume of the nanoparticle, h an applied field in linear response regime, and M_s the saturation magnetization. Here we supposed that the direction of the field is parallel to the anisotropy axes for simplicity. The superparamagnetic relaxation time in zero field for the thermal activation over the energy barrier KV is given by $\tau = \tau_0 \exp(KV/T)$, where τ_0 is a microscopic time.

The occupation probability of one of the two states, in which the superspin is parallel (antiparallel) to the field direction, is denoted by $p_1(t)$ $[1-p_1(t)]$, and is solved by the following master equation:[53]

$$\frac{d}{dt}p_1(t) = -W_{1\to 2}(t)p_1(t) + W_{2\to 1}(t)\{1-p_1(t)\}, \qquad (1)$$

where $W_{1\to 2}(t)$ $[W_{2\to 1}(t)]$ is the transition rate from the state 1 to 2 (2 to 1) at time t. To the leading order in $h(t)$ they are written as

$$W_{1\to 2}(t) = \frac{1}{2}\tau_0^{-1}\exp[-KV/T(t)]\{1 - M_sVh(t)/T(t)\}, \quad (2)$$

$$W_{2\to 1}(t) = \frac{1}{2}\tau_0^{-1}\exp[-KV/T(t)]\{1 + M_sVh(t)/T(t)\}. \quad (3)$$

The above master equation can be solved analytically for any temperatures and field protocols represented by $T(t)$ and $h(t)$ from a given initial condition, and the magnetization of the particle with volume V is given by

$$M(t;V) = [2p_1(t;V) - 1]M_sV. \qquad (4)$$

For example, in the case that $h(t)=h$ and $T(t)=T$, we obtain

$$M(t;V) = M(t=0;V)\exp(-t/\tau) + \frac{(M_sV)^2h}{T}\{1-\exp(-t/\tau)\}, \qquad (5)$$

where $\tau \equiv \tau_0 \exp(KV/T)$. Note that the additional condition $h=0$ leads us to the familiar formulation for the decay of the thermoremanent magnetization.

From Eqs. (1)–(4), we notice that $p_1(t)=1/2$ $[M(t)=0]$ at any t if $p_1(0)=1/2$ and $h(t)=0$. This means that in any *genuine* zero-field-cooled (ZFC) processes starting from $M=0$, $p_1(t)$ is independent of the schedule of temperature change $T(t)$, i.e., no memory is imprinted in the process. Experimentally, a demagnetized initial state is obtained by choosing the starting temperature sufficiently high.

The total magnetization of the nanoparticle system is evaluated by averaging over the volume distribution,

$$\overline{M}(t) = \int dV\, P(V)M(t;V) \equiv \int dV\, M_{\rm spec}(t;V). \qquad (6)$$

Here, the integrand (the M spectrum) denoted as $M_{\rm spec}(t;V)$ plays an important role in the arguments below. For the explicit evaluation of $\overline{M}(t)$, we use a log-normal distribution

$$P(V) = \exp[-\ln(V)^2/(2\gamma^2)]/(\gamma V\sqrt{2\pi}), \qquad (7)$$

where $\gamma=0.6$, and V is measured in units of the average volume $\overline{V}$, which is given by $\exp(\gamma^2/2)$. Although quantitative and some minute qualitative results may depend on the value of γ, the functional form of $P(V)$, and even our basic assumption of the two-state representation, we do not go into such detail here, expecting that our simplest model catches the essence of slow dynamics of superparamagnets.

In the present work the average anisotropic energy $\overline{KV}$ is chosen as the unit of energy as well as that of temperature by setting $k_B=1$. As for the time scale, we suppose that the microscopic time τ_0 for superspins of realistic nanoparticles is around 10^{-9} s, and that a typical experimental time window is around 10^2 s. We therefore investigate our model in the time window around $10^{11}\tau_0$ expecting that it corresponds to typical experimental time scales.

B. ZFC and FC magnetizations

Let us begin our arguments from the most fundamental and well-known protocols, i.e., the measuring processes of the zero-field-cooled magnetization (ZFCM) and the field-cooled magnetization (FCM). In the ZFC process, the system is rapidly cooled to a low temperature in zero field, and then the induced magnetization by an applied field h is measured as the temperature is gradually increased. In the FC process, on the other hand, the system is gradually cooled under h from a sufficiently high temperature so that the system is in equilibrium at the highest temperature. The circles and squares in Fig. 1 represent the ZFCM and FCM observed with heating and cooling rate r of $2.4\times 10^{12}\tau_0$ per tempera-

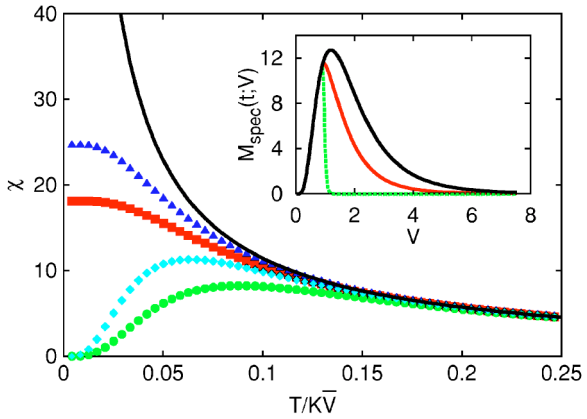

FIG. 1. (Color online) ZFCM and FCM with the cooling rate $r=2.4\times10^{12}\tau_0$ per temperature unit (circles and squares) and those with slower cooling rate $r=2.4\times10^{16}\tau_0$ (diamonds and triangles). The line is the susceptibility in equilibrium (the Curie law). The inset shows the M spectra of the ZFCM, FCM, and the magnetization in equilibrium at $T=0.042$ (from left to right). The cooling rate for ZFCM and FCM is $2.4\times10^{12}\tau_0$.

ture unit.[60] As usually adopted, the peak position of the ZFCM is regarded as the blocking temperature T_B, which is $\simeq 0.088$ for the present process. If the rate r is 10^4 times slower, we obtain $T_B \simeq 0.063$ (diamonds for the ZFCM and triangles for the FCM). If we make r infinitely slow, both the ZFCM and the FCM curves coincide with the one given by the Curie law.

In the inset of Fig. 1 we show the M spectra [the integrand of Eq. (6)] of the ZFCM, FCM, and the magnetization in equilibrium at $T=0.042$ (from left to right). One can clearly see that the parts of the three M spectra for V smaller than a certain value, which we denote as V_B, lie on top of each other. This means that superspins of these small nanoparticles are equilibrated within the characteristic time scale of the cooling and heating process. On the other hand, the M spectrum of the ZFCM at $V \gtrsim V_B$ is zero, indicating that superspins of these larger nanoparticles are still blocked to their initial values. We call V_B the blocking volume which depends strongly (linearly) on T and weakly (logarithmically) on the observation time scale. Also we call superspins of nanoparticles with $V \lesssim V_B$, $V \simeq V_B$, and $V \gtrsim V_B$ *superparamagnetic*, *dynamically active*, and *blocked* or *frozen*, respectively.

In passing we emphasize another characteristic feature of the FCM in superparamagnets; namely, the FCM always increases as the temperature is decreased. This is simply because superspins are blocked (or frozen) in the direction of the field.

C. Aging and memory effects

Let us now consider the thermoremanent-magnetization (TRM) protocol, where we cool the system in a field h at a certain rate, stop the cooling at a measurement temperature T_m, let the system relax for a waiting time of t_w, and then cut the field and observe the magnetization decay. During the FC aging before cutting the field, the parts of the M spectrum for

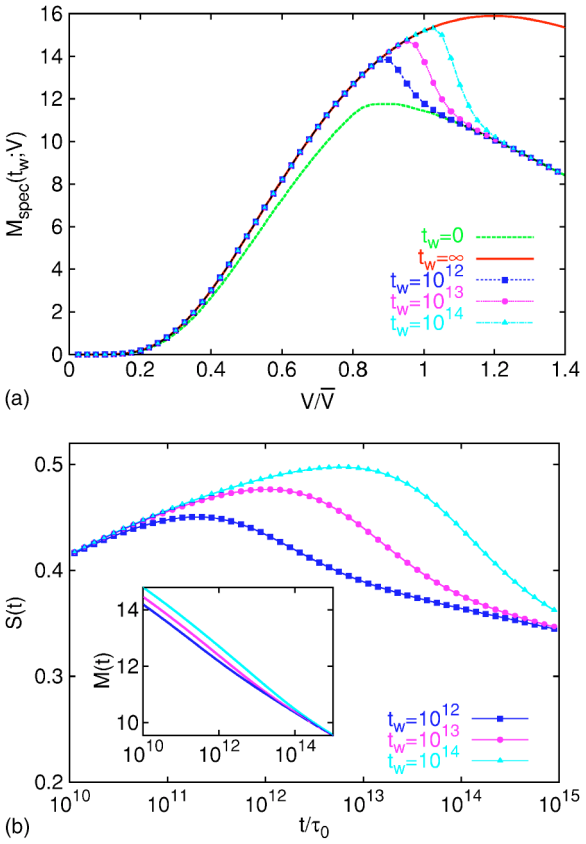

FIG. 2. (Color online) (a) $M_{spec}(t_w;V)$ of the FC process. The system is cooled to $T_m(=0.033)$ at the rate of $2.4\times10^{12}\tau_0$ per temperature unit, and is kept at T_m for t_w. The field is applied in the whole process. (b) Susceptibility $\chi_{TRM}(t,t_w)$ measured in the TRM protocol (inset) and its logarithmic time derivative $S(t) \equiv -d\log\chi_{TRM}(t,t_w)/d\log t$ (main frame) vs t, where t is the elapsed time after the field is cut. The cooling rate and T_m are the same as in (a). In the inset, the corresponding waiting time increases from left to right.

the frozen and superparamagnetic superspins do not change significantly, while that of the dynamically active superspins does change as seen in Fig. 2(a). The peak of the M spectrum shifts to larger volumes with increasing t_w. The peak position appears around V^* where the corresponding relaxation time $\tau_0 \exp(KV^*/T_m)$ is comparable with t_w. This naturally means that the TRM decreases most rapidly when the time t elapsed after the field is cut is nearly equal to t_w. Indeed, Fig. 2(b) shows that the relaxation rate $S(t) \equiv -h^{-1}d\log M/d\log t$ in the TRM protocol has a peak around t_w. Thus we conclude that aging (a t_w dependence) of the TRM does exist even in superparamagnets.

As mentioned in Sec. II A, however, the ZFCM curve is independent of t_w. One may consider that this t_w independence of the ZFCM is a consequence of the simple two-states description of our model. Actually, by considering several competing sources of anisotropy (for instance magnetocrystalline and magnetostatic energy), we can think of a multistate system with some energy levels different from each other. Then, the ZFCM of the model should depend weakly on t_w even if interactions among particles are absent.

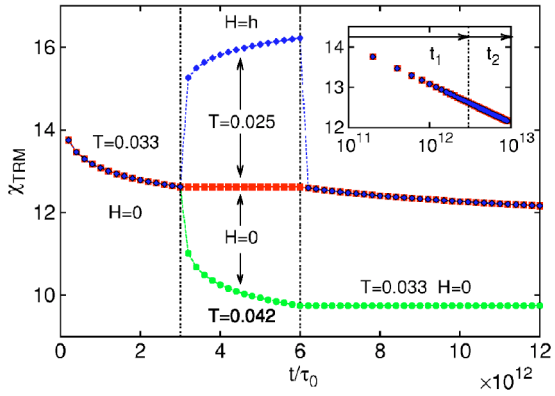

FIG. 3. (Color online) χ_{TRM} vs time using the same protocols as in Figs. 3–5 of Sun *et al.* (Ref. 39). The system is cooled to $T=0.033$ at the rate of $2.4\times10^{13}\tau_0$ per temperature unit in a field which is cut just before recording χ_{TRM}. After a time of $t_1=3\times10^{12}\tau_0$ the temperature is changed. The relaxation at the new temperature is recorded in either $H=0$ or $H=h$ for a period of $t_2=3\times10^{12}\tau_0$. Then the temperature is shifted back to $T=0.033$ and the field is set to zero. In the inset, t_1 and t_3 parts of χ_{TRM} with the negative-temperature cycling are plotted as a function of the total time elapsed at $T=0.033$.

In fact, we will show in Sec. III that the random energy model, which has a huge number of states whose energies are different from each other, exhibits strong aging in genuine ZFC protocols. However, we consider that a significantly small t_{w} dependence of the ZFCM as compared to that of the TRM is one of the characteristic properties of superparamagnets since in ordinary spin glasses, a strong t_{w} dependence is observed not only in the TRM but also in the ZFCM. Therefore, indubitable experimental evidence for spin-glass dynamics in a system can only be found by investigating aging effects in the ZFCM.

From the sum rule for the ZFCM, TRM, and FCM, we find

$$M_{\mathrm{TRM}}(t,t_{\mathrm{w}}) = M_{\mathrm{FC}}(t+t_{\mathrm{w}}) - M_{\mathrm{ZFC}}(t), \tag{8}$$

where we have used the fact that the ZFCM does not depend on t_{w} in our model. This equation tells us that the t_{w} dependence of the TRM in our model is merely a consequence of slow relaxation of the FCM. This is in contrast to ordinary spin glasses where the TRM and the ZFCM strongly depend on t_{w} even if $M_{\mathrm{FC}}(t')$ for $t'\geqslant t_{\mathrm{w}}$ hardly relaxes.[54]

Another important point is that the peak position of the M spectrum in Fig. 2(a) [and the relaxation rate $S(t)$ in Fig. 2(b)] ceases to shift if $t_{\mathrm{w}}\geqslant\tau_0\exp(KV_{\mathrm{peak}}/T_{\mathrm{m}})$, where V_{peak} is the peak position of the M spectrum in equilibrium (its explicit value is around 1.2 in the present case). On the other hand, aging in spin glasses is believed to persist eternally in the thermodynamic limit since the relaxation time diverges below the critical temperature.

After the field is cut in the above-mentioned TRM protocol with $t_{\mathrm{w}}=0$, we may further introduce some cycling processes,[31,39] as shown in Fig. 3. Now let us first consider a negative-temperature cycling in zero field. The temperature is changed as $T_{\mathrm{m}}=0.033\rightarrow T_2=0.025\rightarrow T_{\mathrm{m}}$. Since the blocking volume V_{B} at T_2 is smaller than that at T_{m}, the superspins which were dynamically active at T_{m} are frozen in the second stage at T_2, while the dynamically active superspins at T_2 do not change because they were already equilibrated (depolarized) by the first-stage aging at T_{m}. Hence M_{TRM} does not change at all in the second stage (squares in Fig. 3). The shape of the M spectrum in this stage is essentially the same as that shown in Fig. 5(b), below. After the system comes back to T_{m} the relaxation of M_{TRM} resumes from the value at the end of the first stage. If the field is applied in the second stage of the above protocol, the superparamagnetic and dynamically active superspins at T_2 respond to it. The M spectrum at the end of this stage is essentially the same as that in Fig. 5(c). The induced magnetization in the second stage almost immediately disappears in the last stage at T_{m} since the superspins which carried the excess magnetization are rapidly equilibrated (depolarized) at the higher temperature. In the positive-temperature cycling with $T_2=0.042$ under $h=0$, superspins which are blocked at T_{m} but not at T_2 (i.e., superspins of nanoparticles whose volume is larger than V_{B} at T_{m} but smaller than V_{B} at T_2) are rapidly depolarized in the second stage. They are frozen as depolarized after changing the temperature back to T_{m}, and thus M_{TRM} remains constant at a much smaller value. The significant relaxation is expected to resume at a time scale when the isothermal M_{TRM} at T_{m} reaches this small value. These features have been in fact observed by Sun *et al.*[39] in a permalloy nanoparticle system.

Lastly let us discuss the peculiar memory effect in Fig. 2 of Sun *et al.*[39] They introduce intermittent stops, at T_i, in the FC process and at the same time they cut off the field, let the system relax by a certain period t_i, and then resume the FC process. When the system is reheated after reaching a certain low temperature, the magnetization curve clearly manifests that the system keeps memories imprinted by the preceding FC process. We have applied the same protocol to our simple model of superparamagnets, and have reproduced qualitatively identical results to theirs as shown in Fig. 4.

It is clarified in Fig. 5 that this peculiar memory effect originates from the blocking of superspins by demonstrating the M spectra of some representative instants of the process. After the first stop at $T=T_1$ under $h=0$, the M spectrum of Fig. 5(b) tells us that the blocking volume V_{B1} is around 3.0, namely, the superspins of nanoparticles with $V\lesssim V_{\mathrm{B1}}$ are completely equilibrated (depolarized), while the frozen superspins of nanoparticles with $V\gtrsim V_{\mathrm{B1}}$ are still blocked at $T=T_1$ after the waiting time. As the FC process is resumed, the memory of the first stop at $T=T_1$ is imprinted as a dip at $V\simeq V_{\mathrm{B1}}$ in the M spectrum [Fig. 5(c)], since that part of the M spectrum is well blocked during the aging at significantly lower temperatures than T_1. Similarly, by the second stop at $T=T_2$ and recooling afterward, another dip at $V_{\mathrm{B2}}\simeq1.3$ is imprinted in the M spectrum as seen in Fig. 5(d). In the reheating process, Figs. 5(e) and 5(f) illustrate that the frozen part of the M spectrum melts starting from small V. The consequence is nothing but the memory effect reported by Sun *et al.*

D. Experiments on a superparamagnet

In order to clarify how far our simple model captures the essence of *real* superparamagnets, we perform experiments

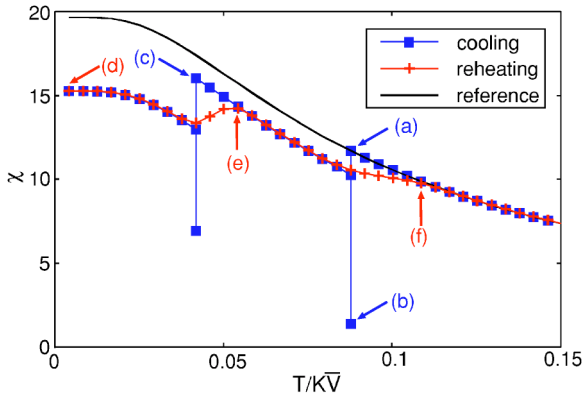

FIG. 4. (Color online) FC susceptibility vs temperature observed in the same protocol as in Fig. 2 of Sun *et al.* (Ref. 39). The field is cut during the intermittent stops of the cooling at $T_1=0.088$ and at $T_2=0.042$ for a period of $10^{14}\tau_0$. The magnetization in zero field after the waiting time is shown although it was not shown by Sun *et al.* The arrows in the figure indicate at which stages during the procedure we measure and show the M spectra in Fig. 5 below. The cooling (and reheating) rate is the same as that in Fig. 3.

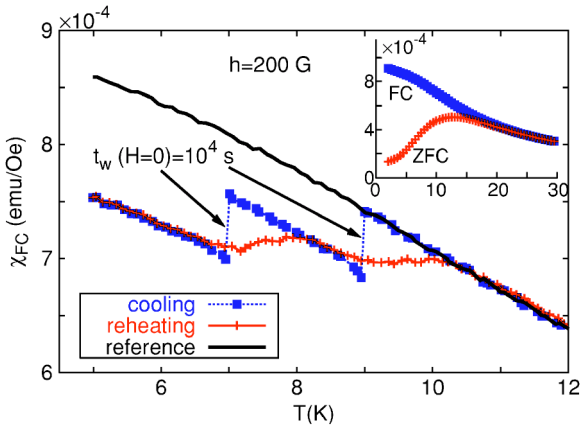

FIG. 6. (Color online) FC susceptibility of ferritin with the same protocol as that in Fig. 4. The field is cut during the intermittent stops of the cooling at $T=9$ and 7 K for 10^4 s at each temperature. The cooling (and reheating) rate is 1.7×10^{-3} K/s. The inset shows the ZFC and the FC susceptibilities vs temperature.

on a *model superparamagnet*, namely, natural horse-spleen ferritin.[43,44] It is an iron-storage protein, and has a spherical cage 8 nm in diameter containing polydispersive cores of antiferromagnetic ferrihydrite.[55,56] Each core has a small magnetic moment of $\sim 300\mu_B$ due to its uncompensated spins.[43,57] Figure 6 shows the result of the memory experiment with the same protocol as that in Fig. 4. It is clear from the figure that this superparamagnet also exhibits the same memory effect as that observed by Sun *et al.* In fact, this memory behavior is also observed in other superparamagnets.[41,42] The FCM without stops is shown in the inset of Fig. 6. We see that the FCM increases monotonically with decreasing temperature. As we discussed in the last paragraph of Sec. II B, this is a typical feature of superparamagnets.

Figure 7 shows relaxation of the TRM susceptibility with the same protocol as that in Fig. 2(b). We clearly see that the TRM exhibits a similar t_w dependence to that in our simple model of superparamagnets. We have also checked a tendency that the peak of the relaxation rate $S(t) \equiv -h^{-1}d\log M/d\log t$ shifts to larger times with increasing t_w, although the data are a bit too noisy to clarify whether the peak is located around t_w or not.

We have also done a memory experiment in the *genuine* ZFC protocol.[54] In this experiment, we measure χ_{ZFC} which includes intermittent stops in the ZFC process and χ_{ZFC}^{ref} without such stops. The stopping temperatures are 9 and 7 K, and the period of intermittence is 10^4 s at each temperature. Note

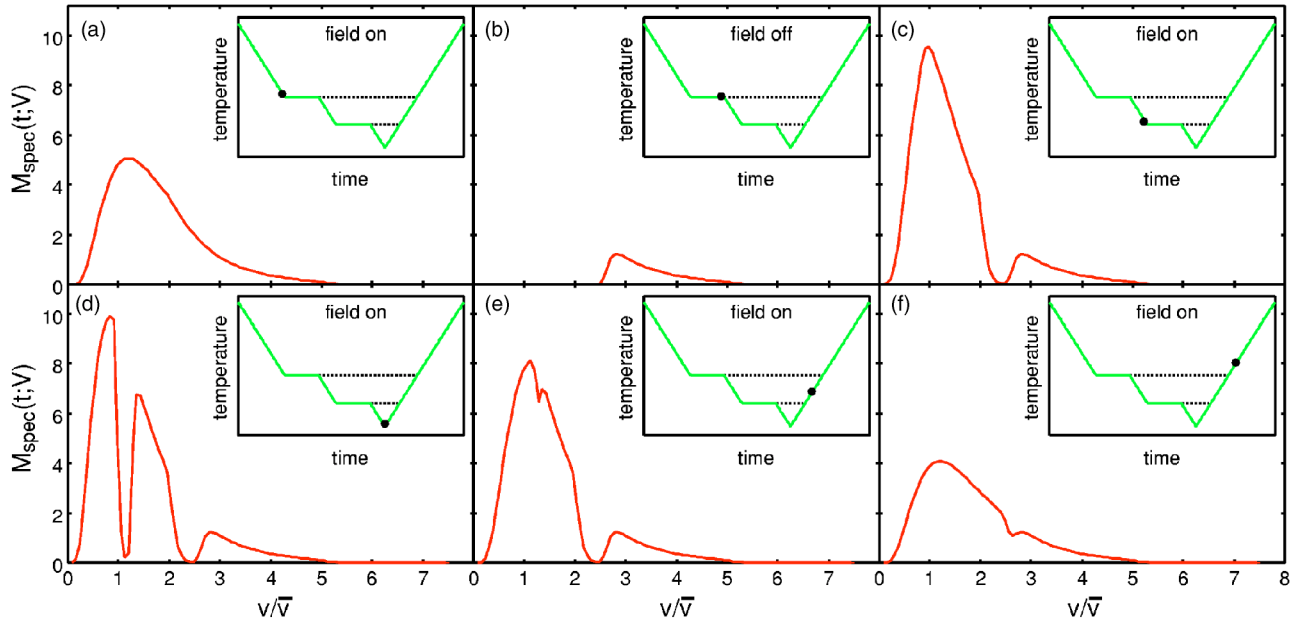

FIG. 5. (Color online) M spectra at six representative states which are indicated in Fig. 4 by arrows. The point in each inset also shows the time of the measurement.

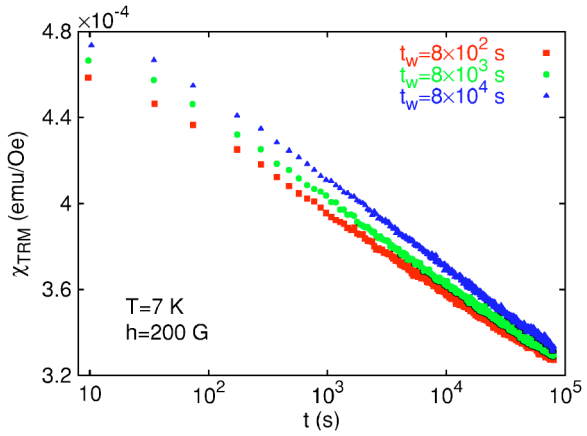

FIG. 7. (Color online) Relaxation of the TRM susceptibility of the ferritin. After the system is cooled to $T=7.0$ K under a 200 Oe field at a rate of 0.17 K/s, it is kept at the temperature under the field for t_w, and then the field is cut and the magnetization decay is measured as a function of the elapsed time t after the field is cut. The waiting time t_w is 8×10^2, 8×10^3, and 8×10^4 (from left to right).

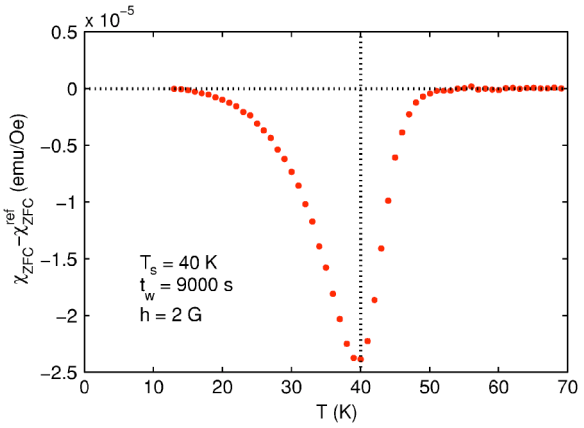

FIG. 9. (Color online) Difference of the ZFC susceptibility of the Fe_3N system. The ZFC process is intermitted at $T=40$ K for 9000 s in the measurement of χ_{ZFC}, while χ_{ZFC}^{ref} is measured without such a stop. The cooling rate is 0.1 K/s, and the reheating rate is 0.01 K/s.

that the stopping temperatures are well below the blocking temperature $T_B \approx 13$ K (see the inset of Fig. 6). The cooling (and reheating) rate is the same as that in Fig. 6. The result of the experiment is that there is no significant difference between χ_{ZFC} and χ_{ZFC}^{ref} at any temperature (not shown), i.e., no memory is imprinted by the aging under zero field. This is also the expected result for superparamagnets.

III. SLOW DYNAMICS IN SUPERSPIN GLASSES

Various memory experiments are performed on a dense Fe_3N ferromagnetic nanoparticle system which has been shown to be a superspin glass.[29,37,45,46] Figure 8 shows the result of the memory experiment following the same protocol as that in Fig. 4. At the intermittent stops of the FC process, while the field is set to zero, the value of the magnetization decreases. On the subsequent reheating, the magnetization value in the preceding cooling process is recovered, for each stop, at a temperature a bit above that of the stop. At a glance, the memory effect in this superspin glass is qualitatively the same as that in superparamagnets indicating a similar origin of the effect. Another interesting observation in Fig. 8 is that the FCM of the Fe_3N system after resuming the cooling behaves almost in parallel to the FCM without the intermittent stops (reference curve) though its absolute magnitude is significantly smaller than the latter. This feature is also seen for the superparamagnets as shown in Figs. 4 and 6, and so it suggests that the mechanism behind the memory effect is also common.

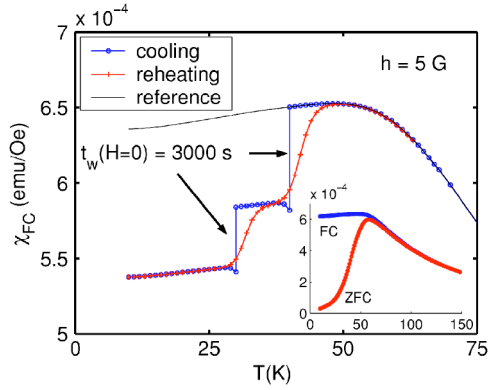

FIG. 8. (Color online) FC susceptibility of the Fe_3N system with the same protocol as that in Fig. 4. The critical temperature of the sample is around 60 K (Ref. 37). The field is cut during the intermittent stops of the cooling at $T=40$ and 30 K for 3000 s at each temperature. The cooling (and reheating) rate is 0.01 K/s. The inset shows the ZFC and the FC susceptibilities vs temperature.

Now let us go into further comparisons between the results so far obtained for the superparamagnets and those for the superspin glass. One significant difference between the two is seen in the behavior of the reference FCM without the intermittent stops. The FCM of the Fe_3N system does not increase but even decreases as the temperature is decreased. According to the argument in the last paragraph of Sec. II B, this implies that the Fe_3N system is in fact not a superparamagnet also in this respect. Actually the nearly constant FCM is considered to be a typical property of ordinary spin glasses. A further important phenomenon which is peculiar to superspin glasses is the memory effect in the genuine ZFC protocol. Figure 9 shows an experimental result of the Fe_3N system where the difference between the ZFCM's with and without an intermittent stop at T_s in the cooling process is presented. The difference is clearly observed as a dip at $T \simeq T_s$.

Now let us discuss possible theoretical interpretations of these experimental results. The first theoretical model we consider is the random energy model (REM).[50–52] The REM consists of a huge number of states. The barrier energy E_B, which the system needs to overcome in order to go to a new state, is assigned to each state randomly and independently according to the exponential distribution $\rho(E_B) = 1/T_c \exp[-E_B/T_c]$. Since the average relaxation time $\langle\tau\rangle = \int_0^\infty dE_B \rho(E_B)\tau_0 \exp(E_B/T)$ diverges below T_c, the REM

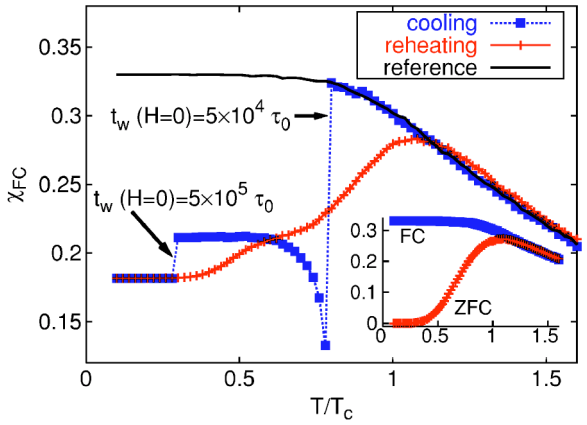

FIG. 10. (Color online) FC susceptibility of the REM with the same protocol as that in Fig. 4. The field is cut during the intermittent stops of the cooling at $T=0.8T_c$ for $5\times10^4\tau_0$ and at $T=0.3T_c$ for $5\times10^5\tau_0$, where τ_0 is the microscopic time of the model. The cooling (and reheating) rate is $2\times10^{-5}T_c/\tau_0$. The inset shows the ZFC and the FC susceptibilities vs temperature.

shows various memory and aging behaviors in the low-temperature phase.[51,52,58] Let us now see to what extent the experimental results shown in this section are reproducible by the REM. First, Fig. 10 shows the result with the same protocol as that in Fig. 4. The result is qualitatively rather similar to that of the Fe_3N system shown in Fig. 8. In particular, it should be emphasized that the flatness of the FCM below the critical temperature, which cannot be captured by our simple model of superparamagnets, is reproduced in the REM. Second, Fig. 11 shows the result of simulation which corresponds to the ZFC memory experiment in Fig. 9. Again, the result is qualitatively very similar to that in the experiment. A crucial property of the REM to understand this result is that the system goes into deeper and deeper states with higher and higher energy barriers as time progresses.[51,59] Therefore, the typical energy barrier of the state in which the system is blocked depends on how long the system has been aged at a low temperature. Since it is more difficult for the

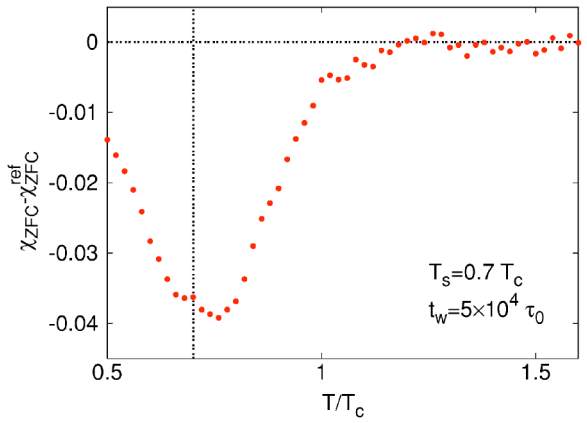

FIG. 11. (Color online) Difference of the ZFC susceptibility of the the REM. The ZFC process is intermitted at $T=0.7T_c$ for $5\times10^4\tau_0$ in the measurement of χ_{ZFC}, while χ_{ZFC}^{ref} is measured without such a stop. The cooling (and reheating) rate is the same as that in Fig. 9.

system blocked in a state with a higher energy barrier to respond to the field, the difference of the typical energy barrier of the state in which the system is blocked with and without intermittent stop on cooling causes the dip in Fig. 11.

We have seen that the experimental results are well reproduced by the REM. However, the link between each state in the REM and an actual spin configuration in the system is not so clear. On the other hand, the droplet theory[20,48] gives some insight into spin configurations in the (nonequilibrium) dynamics of real spin glasses. For example, after a spin glass is rapidly quenched in a field h to a temperature T below T_c, spin-glass domains, or clusters, which are in local equilibrium with respect to (T,h) are considered to grow. At a certain instance t after the quench, clusters with various volumes V_{cluster} or linear sizes $L(\sim V_{\text{cluster}}^{1/d})$ exist. We may think of their distribution $P(t;V_{\text{cluster}})$ analogously to $P(V)$ in the previous section. Furthermore, in the droplet theory, each cluster of a size L is considered to flip by a thermal activation process whose mean energy barrier B_L is a function of L ($B_L\sim L^{\psi}$ in the original droplet theory[20]). The thermally activated process governs the response of clusters to an applied field. This situation is rather similar to the two-state description of the superparamagnet, and we may expect that the magnetization of the spin glass is also described by Eq. (6), though the functional form of $M(t;V)$ has to be properly modified and $P(V)$ has to be replaced by a time-dependent distribution $P(t;V_{\text{cluster}})$. We also note that the above argument on an atomic spin glass can be directly applied to a superspin glass if an atomic spin in the former is replaced by a superspin in the latter.

An interesting prediction of the droplet theory is the instability of the equilibrium spin-glass phase under a static magnetic field h of any strength. This is one of the fundamental issues which has been debated since the early stage of the spin-glass study and has not been settled yet. Quite recently, in numerical analysis of the field-shift aging protocol, one of the present authors (H.T.) and Hukushima[49] have found results that strongly support the prediction of the droplet theory. Here let us argue about our experimental results on the superspin glass from this point of view, namely, the FCM measured at $T<T_c$ is not an equilibrium property under h but due to the blocking of superspin clusters introduced above.

As noted before, the FCM of a superparamagnet increases with decreasing T. That of the present superspin glass, on the other hand, is nearly constant at $T\lesssim T_c$ as seen in the inset of Fig. 8. The latter is naturally attributed to the expected fact that the free-energy difference between the two states of a superspin cluster is given not only by the Zeeman energy but also by the residual interactions between the cluster and its surroundings (the stiffness energy of a cluster in the droplet theory). If the field strength is sufficiently small, which is the case of the present interest, the latter certainly dominates the Zeeman energy. Therefore, when the cluster is blocked, its magnetization points either parallel or antiparallel to the field direction. Consequently the branch of the FCM at $T\lesssim T_c$ in Fig. 8 becomes nearly constant when the temperature is decreased.

By further inspection of Fig. 1 and the inset of Fig. 8 we notice that the FCM of a superparamagnet changes rather

smoothly around the blocking temperature, while that of the superspin glass exhibits a kinklike shape at $T \sim T_c$. The latter can be attributed to the time development of $P(t; V_{\text{cluster}})$ which is absent in a superparamagnet. In fact, in the droplet theory, the rates of growth of the spin-glass clusters and so of their barrier energy are expected to be most sensitive to a small change in temperature at $T \simeq T_c$, since they are governed by the critical dynamics associated with the spin-glass transition at $T = T_c$ under $h = 0$. Consequently, even a small temperature decrease at this temperature range gives rise to an apparently sharper blocking of superspin clusters. At significantly lower temperatures than T_c, the thermal activation process governs dynamics of superspins and yields an almost constant FCM as described just above.

Let us turn to memory effects in the genuine ZFC protocol, which are not observed in superparamagnets. As we mentioned above, at $T \lesssim T_c$, sizes of clusters are growing as time elapses which gives rise to a history dependence of $P(t; V_{\text{cluster}})$ in the language of our two-state model. Since the change of $P(t; V_{\text{cluster}})$ proceeds even in a vanishing field, memory effects are observed even in the genuine ZFC protocol.

Lastly one comment is in order on possible differences in the slow dynamics of superspin glasses and atomic spin glasses. As mentioned above, qualitative aspects of the two are considered to be almost common to each other. Quantitatively, however, the unit time of a superspin flip depends on T and is much larger than the temperature-independent atomic-spin flip time. This difference often causes apparent qualitative differences in the nonequilibrium phenomena in the two spin glasses. The most interesting phenomenon among them is *rejuvenation* arising from the chaotic nature of equilibrium spin-glass states.[18–21] The rejuvenation is more easily seen in longer time scales in units of the moment or spin flip time; namely, within a common experimental time window of $10^1 - 10^5$ s, the effect is harder to observe in superspin glasses than in atomic spin glasses. This problem is investigated in a separate paper.[46]

IV. SUMMARY

We have studied dynamics of superparamagnets by investigating a simplified two-state model analytically and ferritin experimentally. As a consequence, we have found that (a) the TRM exhibits a t_w dependence, and the logarithmic time derivative of $\chi_{\text{TRM}}(t, t_w)$ has a peak around $t \approx t_w$, as observed in spin glasses; (b) all the experimental results reported by Sun *et al.*[39] are qualitatively reproducible. In superparamagnets, these aging and memory effects originate solely from a broad distribution of relaxation times which comes from that of the anisotropy energy barriers. The mechanism of these results is well understood by investigating the time dependence of the M spectrum [the integrand in Eq. (6)]. Thus the aging and memory effects (a) and (b) are not a sufficient proof for the existence of spin-glass dynamics.

We have also studied aging and memory effects in a dense Fe_3N nanoparticle system (a *superspin glass*) experimentally. By comparing the results with those for superparamagnets, the following differences have been found: (1) The FCM of the Fe_3N system does not increase but even decreases as the temperature is decreased, while the FCM of superparamagnets always increases with decreasing temperature. (2) In the Fe_3N system, the genuine ZFCM also depends on the waiting time. Such a t_w dependence in the ZFCM is hardly expected in superparamagnets. From the viewpoint of (1), we consider that the permalloy nanoparticle system studied by Sun *et al.* is closer to a superparamagnet, while the Fe_3N system studied in the present work and the Co-Fe nanoparticle system studied by Sahoo *et al.*[31,32,38] are closer to a superspin glass. Lastly, we have argued that these two aspects peculiar to superspin glasses are qualitatively reproduced by the random energy model, and are well interpreted by the droplet theory in the field of spin-glass study.

In conclusion, similarities as well as crucial differences in aging and memory effects in superparamagnets and superspin glasses have been clarified. In order to distinguish the two types of slow dynamics we have to choose appropriate aging protocols such as a ZFC process with intermittent stops of the cooling properly scheduled.

ACKNOWLEDGMENTS

M.S. and P.E.J. acknowledge financial support from the Japan Society for the Promotion of Science. The present work is supported by a Grant-in-Aid for Scientific Research Program (No. 14540351) and NAREGI Nanoscience Project from the Ministry of Education, Culture, Sports, Science and Technology.

[1] L. C. E. Struik, *Physical Aging in Amorphous Polymers and other Materials* (Elsevier, Houston, 1978).
[2] L. Lundgren, P. Svedlindh, P. Nordblad, and O. Beckman, Phys. Rev. Lett. **51**, 911 (1983).
[3] L. Bellon, S. Ciliberto, and C. Laroche, cond-mat/9905160 (unpublished).
[4] L. Bellon, S. Ciliberto, and C. Laroche, Europhys. Lett. **51**, 551 (2000).
[5] C. Rossel, Y. Maeno, and I. Morgenstern, Phys. Rev. Lett. **62**, 681 (1989).
[6] C. Josserand, A. V. Tkachenko, D. M. Mueth, and H. M. Jaeger, Phys. Rev. Lett. **85**, 3632 (2000).
[7] E. Vincent, J. P. Bouchaud, J. Hammann, and F. Lefloch, Philos. Mag. B **71**, 489 (1995).
[8] P. Nordblad and P. Svedlindh, in *Spin Glasses and Random Fields*, edited by A. P. Young (World Scientific, Singapore, 1998).
[9] K. Jonason, E. Vincent, J. Hammann, J. P. Bouchaud, and P. Nordblad, Phys. Rev. Lett. **81**, 3243 (1998).
[10] L. F. Cugliandolo and J. Kurchan, Phys. Rev. Lett. **71**, 173

(1993).
[11] J.-P. Bouchaud, L. Cugliandolo, J. Kurchan, and M. Mézard, in *Spin Glasses and Random Fields* (Ref. 8).
[12] H. Yoshino, A. Lemaître, and J.-P. Bouchaud, Eur. Phys. J. B **20**, 367 (2000).
[13] M. Sasaki and K. Nemoto, J. Phys. Soc. Jpn. **69**, 2283 (2000).
[14] T. Komori, H. Yoshino, and H. Takayama, J. Phys. Soc. Jpn. **69** Suppl. A, 228 (2000).
[15] L. Berthier and J.-P. Bouchaud, Phys. Rev. B **66**, 054404 (2002).
[16] M. Mézard, G. Parisi, N. Sourlas, G. Toulouse, and M. A. Virasoro, J. Phys. (France) **45**, 843 (1984).
[17] M. Mézard, G. Parisi, N. Sourlas, G. Toulouse, and M. Virasoro, Phys. Rev. Lett. **52**, 1156 (1984).
[18] D. S. Fisher and D. A. Huse, Phys. Rev. Lett. **56**, 1601 (1986).
[19] A. J. Bray and M. A. Moore, Phys. Rev. Lett. **58**, 57 (1987).
[20] D. S. Fisher and D. A. Huse, Phys. Rev. B **38**, 386 (1988).
[21] M. Sasaki, K. Hukushima, H. Yoshino, and H. Takayama, cond-mat/0411138 (unpublished).
[22] A. Wills, V. Dupuis, E. Vincent, J. Hammann, and R. Calemczuk, Phys. Rev. B **62**, R9264 (2000).
[23] V. Dupuis, E. Vincent, J. Hammann, J. E. Greedan, and A. S. Wills, J. Appl. Phys. **91**, 8384 (2002).
[24] R. Mathieu, P. Svedlindh, and P. Nordblad, Europhys. Lett. **52**, 441 (2000).
[25] F. Alberich, P. Doussineau, and A. Levelut, J. Phys. I **7**, 329 (1997).
[26] F. Alberici-Kious, J. P. Bouchaud, L. F. Cugliandolo, P. Doussineau, and A. Levelut, Phys. Rev. Lett. **81**, 4987 (1998).
[27] R. L. Leheny and S. R. Nagel, Phys. Rev. B **57**, 5154 (1998).
[28] T. Jonsson, J. Mattsson, C. Djurberg, F. A. Khan, P. Nordblad, and P. Svedlindh, Phys. Rev. Lett. **75**, 4138 (1995).
[29] H. Mamiya, I. Nakatani, and T. Furubayashi, Phys. Rev. Lett. **82**, 4332 (1999).
[30] P. Jönsson, M. F. Hansen, and P. Nordblad, Phys. Rev. B **61**, 1261 (2000).
[31] S. Sahoo, O. Petracic, C. Binek, W. Kleemann, J. B. Sousa, S. Cardoso, and P. P. Freitas, J. Phys.: Condens. Matter **14**, 6729 (2002).
[32] S. Sahoo, O. Petracic, W. Kleemann, P. Nordblad, S. Cardoso, and P. P. Freitas, Phys. Rev. B **67**, 214422 (2003).
[33] P. E. Jönsson, Adv. Chem. Phys. **128**, 191 (2004).
[34] X. Batlle and A. Labarta, J. Phys. D **35**, R15 (2002).
[35] W. Luo, S. R. Nagel, T. F. Rosenbaum, and R. E. Rosensweig, Phys. Rev. Lett. **67**, 2721 (1991).
[36] T. Jonsson, P. Svedlindh, and M. F. Hansen, Phys. Rev. Lett. **81**, 3976 (1998).
[37] H. Mamiya and I. Nakatani, Nanostruct. Mater. **12**, 859 (1999).
[38] S. Sahoo, O. Petracic, C. Binek, W. Kleemann, J. B. Sousa, S. Cardoso, and P. P. Freitas, Phys. Rev. B **65**, 134406 (2002).
[39] Y. Sun, M. B. Salamon, K. Garnier, and R. S. Averback, Phys. Rev. Lett. **91**, 167206 (2003).
[40] M. Sasaki, P. E. Jönsson, H. Takayama, and P. Nordblad, Phys. Rev. Lett. **93**, 139701 (2004).
[41] R. K. Zheng and X. X. Zhang, cond-mat/0403368 (unpublished).
[42] S. Chakravarty, A. Frydman, M. Bandyopadhyay, S. Dattagupta, and S. Sengupta, Phys. Rev. Lett. **93**, 139702 (2004).
[43] S. H. Kilcoyne and R. Cywinski, J. Magn. Magn. Mater. **140-144**, 1466 (1995).
[44] H. Mamiya, I. Nakatani, and T. Furubayashi, Phys. Rev. Lett. **88**, 067202 (2002).
[45] H. Mamiya, I. Nakatani, and T. Furubayashi, Phys. Rev. Lett. **80**, 177 (1998).
[46] P. E. Jönsson, H. Yoshino, H. Mamiya, and H. Takayama, preceding paper, Phys. Rev. B **71**, 104404 (2005).
[47] G. Parisi, Phys. Rev. Lett. **50**, 1946 (1983), and references therein.
[48] D. S. Fisher and D. A. Huse, Phys. Rev. B **38**, 373 (1988).
[49] H. Takayama and K. Hukushima, J. Phys. Soc. Jpn. **73**, 2077 (2004).
[50] B. Derrida, Phys. Rev. B **24**, 2613 (1981).
[51] J. P. Bouchaud, J. Phys. I **2**, 1705 (1992).
[52] J.-P. Bouchaud and D. Dean, J. Phys. I **5**, 265 (1995).
[53] I. Klik, C.-R. Chang, and J. Lee, J. Appl. Phys. **75**, 5487 (1994).
[54] R. Mathieu, P. Jönsson, D. N. H. Nam, and P. Nordblad, Phys. Rev. B **63**, 092401 (2001).
[55] D. D. Awschalom, J. F. Smyth, G. Grinstein, D. P. DiVincenzo, and D. Loss, Phys. Rev. Lett. **68**, 3092 (1992).
[56] P. M. Harrison, F. A. Fischbach, T. G. Hoy, and G. H. Haggis, Nature (London) **216**, 1188 (1967).
[57] S. A. Makhlouf, F. T. Parker, and A. E. Berkowitz, Phys. Rev. B **55**, R14 717 (1997).
[58] M. Sasaki and K. Nemoto, J. Phys. Soc. Jpn. **69**, 3045 (2000).
[59] M. Sasaki and K. Nemoto, J. Phys. Soc. Jpn. **69**, 2642 (2000).
[60] More explicitly, the master equation (1) is solved by changing the temperature stepwise with a step of $\Delta T = 4.2 \times 10^{-3}$ and at each temperature we let the system relax for a period of $\Delta t = 1.0 \times 10^{10} \tau_0$.